4

Probabilistic Projections of High-Tide Flooding for the State of Maryland in the 21st Century

Ming Li, Fan Zhang, Yijun Guo

University of Maryland Center for Environmental Science, Cambridge, MD, USA

Xiaohong Wang

Salisbury University, Salisbury, MD, USA

CONTENTS

4.1 Introduction

The small area occupied by the coastal zone belies its importance to human affairs and the potential risks posed by climate change. Humans are concentrated in the coastal zone; three-quarters of the global population lives within 50 km of the sea and 50% of the US population lives within 50 miles (∼80 km) of the sea. Climate change is expected to increase the rate of sea-level rise and coastal inundation (Church and Clark, 2013), putting coastal communities in jeopardy of significant property damage, sociocultural and economic disruption, and loss of life. The number of medium-to-large coastal municipalities in

the United States affected by flooding is estimated to exceed 33 in 2050 and 90 in 2100 (Kulp and Strauss, 2017). Globally, 0.2%–4.6% of the population is expected to be flooded annually in 2100 under 0.25–1.23 m of global mean sea level rise, with expected annual losses of 0.3%–9.3% of global gross domestic product (Hinkel et al, 2014). New elevation data triple estimates of global vulnerability to sea level rise and coastal flooding: about 340/630 million people will live in land below annual flood level by 2050/2100 (Kulp and Strauss, 2019). Therefore, there is an urgency to quantify the flooding risks faced by coastal communities, their resilience to rising sea levels, and what should be done to reduce the coastal risks.

Maryland, with over 3000 miles (4828 km) of tidal shoreline along both the Chesapeake Bay and the state's Atlantic Ocean shoreline, is highly vulnerable to sea level rise. Recurrent flooding is already a major problem in Chesapeake Bay (Mitchell et al, 2013) and will likely become more frequent in the future as sea level rises (Spanger-Siegfried et al, 2014). For example, "nuisance" tidal flooding that occurred just a very few days per year in Annapolis in the 1950s now occurs 40 or more days per year (Boesch et al, 2018).

Tide gauge records and satellite altimetry reveal that global-mean sea level (GSML) rose at a rate of 1.2 ± 0.2 mm yr^{-1} between 1900 and 1990 and at a much faster rate of 3.0 ± 0.7 mm yr^{-1} between 1993 and 2012 (Church and White, 2011, Dangendorf et al, 2017, Hay et al, 2015). The rate of sea level rise is accelerating in the 21st century. According to IPCC AR5 (Fifth Assessment Report of the Intergovernmental Panel on Climate Change), GMSL will rise 0.52–0.98 m by 2100 for the highest emission scenario considered—Representative Concentration Pathway RCP 8.5 (Church and Clark, 2013). Probabilistic sea level projections suggest a very likely (90% probability) GMSL rise of 0.5–1.2 m under RCP 8.5 (Kopp et al, 2014). If the rapid collapse of Antarctic ice sheet as projected in some climate models is taken into consideration, the median projected GMSL for 2100 will increase from 0.79 to 1.46 m under RCP 8.5 (Kopp et al, 2017). (For an overview of climate models, see Chapter 1.)

Tide-gauge records in Chesapeake Bay show that sea levels rose by 3–4 mm per year over the 20th century (Zervas, 2001, 2009), twice that of the global average. Land subsidence associated with glacial isostatic adjustment is a major contributor to the high relative sea level rise in the Bay (Miller et al, 2013). Ocean dynamics, arising from changing ocean circulation, may also contribute to higher sea levels at the coast. The weakening of the Gulf Stream over the past decade may have contributed to the higher rates of sea level rise along the Mid-Atlantic coast (Ezer et al, 2013, Kopp, 2013, Sallenger et al, 2012). However, recent analysis showed that sea level declined north of Cape Hatteras between 2010 and 2015, and this decline was caused by an increase in atmospheric pressure combined with shifting wind patterns (Domingues et al, 2018).

With respect to coastal inundation, the height of the highest waters, the sum of local mean sea level and tidal amplitude, is more relevant than the mean

sea level alone. Müller et al (2011) showed that the response of the oceans to tidal forces changed significantly during the last century. Flick et al (2003) examined long-term records at US tide gauges and found significant changes in the tidal range. Semi-enclosed bays such as the Bay of Fundy have natural resonance periods that are close to those for semidiurnal or diurnal tides. In these bays, tide at the head of the bay is greatly amplified as compared to that at the mouth (Garrett, 1972). The resonant period in Chesapeake Bay is about 48 hours. Raising sea level by 1 m shortens it to 36 hours, moves diurnal tides inside the resonance band, and increases tidal ranges in the upper Bay (Zhong et al, 2008). Similar results are found for Delaware Bay: tidal ranges in the upper part increased 100% over the past 4000 years (Hall et al, 2013). However, such calculations ignore the fact that flooding of adjacent low-lying areas introduces frictional, intertidal regions that may serve as energy sinks for incoming tidal waves (Holleman and Stacey, 2014). While sea level rise is accompanied by larger tidal ranges in the Bay of Fundy due to steep rocky coastlines (Greenberg et al, 2012), net tidal amplification in most areas of San Francisco is predicted to be lower in most sea level rise scenarios because many low-lying areas around the northern branch of San Francisco Bay are tidal marshlands (Holleman and Stacey, 2014). Similarly, Lee et al (2017) found that tidal ranges in the upper reaches of Chesapeake and Delaware Bays decrease with sea level rise if the low-lying land, consisting mostly of salt marshes and agricultural fields, is allowed to flood. Therefore, it is important to consider tidal response to sea level rise when projecting flooding in the future climate. The peak tidal sea level is not simply a linear sum of sea level rise and historical tidal height.

There are two approaches to generating sea level rise projections. One develops scenarios spanning a range of possible future scenarios (Sweet and Park, 2014). The other estimates the probability of future sea level changes, either through a central projection with an associated range or through a probability distribution. Kopp et al (2014) synthesized several lines of evidence to produce probability distributions for global and local sea level changes. The probability distribution of relative sea level rise over 2000 is provided over time and for three greenhouse gas emissions pathways or Representative Concentration Pathways (RCP): Growing Emissions (RCP 8.5), Stabilized Emissions (RCP 4.5), and meeting the Paris Agreement (RCP 2.6). This framework has been adopted by California (Griggs et al, 2017), Oregon (Dalton et al, 2017), Washington, and most recently Maryland (Boesch et al, 2018). The likely range (66% chance) of sea level rise in Maryland between 2000 and 2050 is 0.24 to 0.48 m, with 5% chance exceeding 0.61 m and 1% chance exceeding 0.70 m (Boesch et al, 2018, Figure 4.1). Later this century, sea level rise rates are highly sensitive to the emission pathway. Between 2000 and 2100, the likely range for the relative sea level rise in Maryland is 0.36 to 0.91 m under RCP 2.6, 0.49 to 1.04 m under RCP 4.5, and is 0.61 to 1.28 m under RCP 8.5 (Figures 4.1a and 4.1b).

The probabilistic sea level projection is the most appropriate approach for use in planning and regulation, infrastructure siting, design, etc. However,
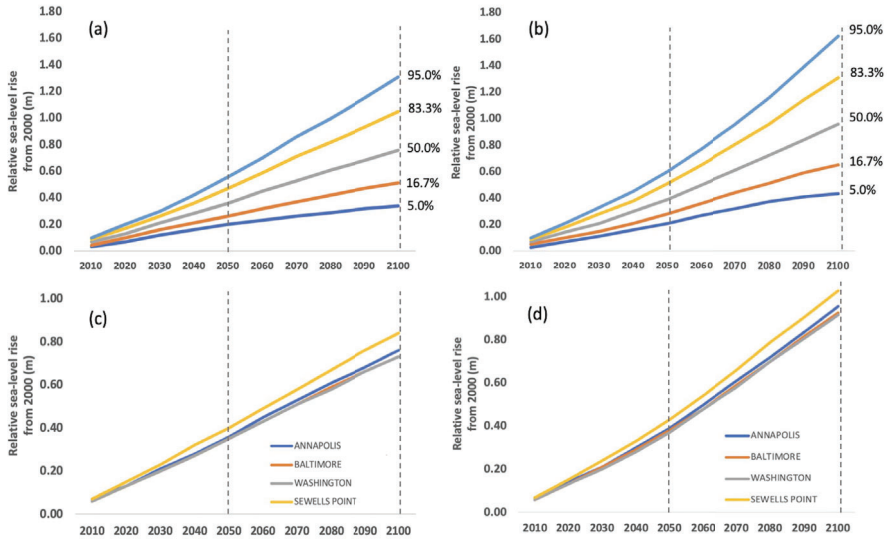
FIGURE 4.1: Probabilistic projections of the relative sea level rise in Annapolis under climate change scenario RCP 4.5 (a) and RCP 8.5 (b). Median projections of the relative sea level rise in Chesapeake Bay under RCP 4.5 (c) and 8.5 (d).

these sea level rise predictions must be projected onto low-lying land areas in order to assess the flooding risks faced by coastal communities. Projections of sea level rise onto land areas were mostly based on static images (e.g., bathtub approach) and did not consider dynamical processes of tides in rising seas. These graphic products may have underestimated the inundation risks faced by coastal community and infrastructure. Statistical approaches were developed to characterize coastal flood risk by using long-term sea level observations at tidal gauges and superimposing the time series with the sea level rise projected for the future climate (Ghanbari et al, 2019, Moftakhari et al, 2015). These analyses led to useful estimates of flood frequency at certain coastal locations but did not provide a direct estimate of the flooded land areas. To account for the full dynamic effect of sea level rise on coastal inundation, an ocean model capable of simulating tides and currents in rising seas is required.

In this study we used a regional ocean model to examine flooding at high tides around Chesapeake Bay, especially over low-lying land areas in the State of Maryland. Three sites were selected as focus studies areas: the City of Baltimore and City of Annapolis are the two largest cities in Maryland; the Dorchester County on the Eastern Shore of Maryland is among the most vulnerable rural areas to sea level rise. Our goal is to produce a probabilistic projection of high tide flooding in 2050 and 2100, and develop dynamics-based inundation

graphics that can prepare coastal communities for the rising inundation risks in the 21st century.

4.2   Methods

To assess the impacts of sea level rise on tidal water levels and coastal inundation in the 21st century, we used the Finite Volume Coastal Ocean Model (FVCOM) and forced it with the probabilistic projections for the relative sea level rise in Chesapeake Bay.

4.2.1   Regional ocean model

The unstructured-grid FVCOM was used to simulate tidal flows and intertidal flooding over low-lying land (Chen et al, 2003, 2006). The model domain covers Chesapeake Bay and the eastern US continental shelf (Figure 4.2a). The horizontal resolution ranges from ∼1 km in the inner shelf to ∼10 km near the open boundaries. The model resolves Chesapeake Bay and its surrounding lands (up to 5 m height above the current mean sea level) at a resolution of 0.2–1.0 km. Finer resolutions are placed over the City of Baltimore, City of Annapolis (5–10 m) and the Dorchester County on the rural eastern shore of Maryland (100–200 m), three focus areas in this study. The model is run in three-dimensional barotropic mode in which temperature and salinity are kept constant. In the vertical direction, five sigma layers are used. At the offshore open boundary, the tidal sea level is prescribed using ten tidal constituents according to the Oregon State University global tidal model TOPEX/POSEIDON 7.1 (Egbert and Erofeeva, 2002). A quadratic stress is exerted at the bed, with the bottom roughness height set to be 2 mm in Chesapeake Bay and 2 cm on the adjacent shelf (Lee et al, 2017). As a simplification the roughness heights are assumed to be the same between the sea beds and the surrounding lands.

   To simulate overland inundation, coastal lands up to 5 m above the mean sea level are included in the model domain. High-resolution (10 m horizontal resolution) digital elevation data in land areas surrounding Chesapeake Bay are obtained from US Geological Survey National Elevation Data Set (Gesch, 2009). Fine-resolution LIDAR data,[1] with a horizontal resolution of 1 foot (∼0.3 m) and a vertical resolution of 1 cm, are used for the digital elevation over Maryland. Bathymetry data are acquired from the NOAA 1 arc-second resolution Bathymetric Digital Elevation Model in the estuary, the 3 arc-second Coastal Relief Model on the continental shelf, and the 1 arc-minute ETOPO1 Global Relief Model in the deep ocean (Amante and Eakins,

---

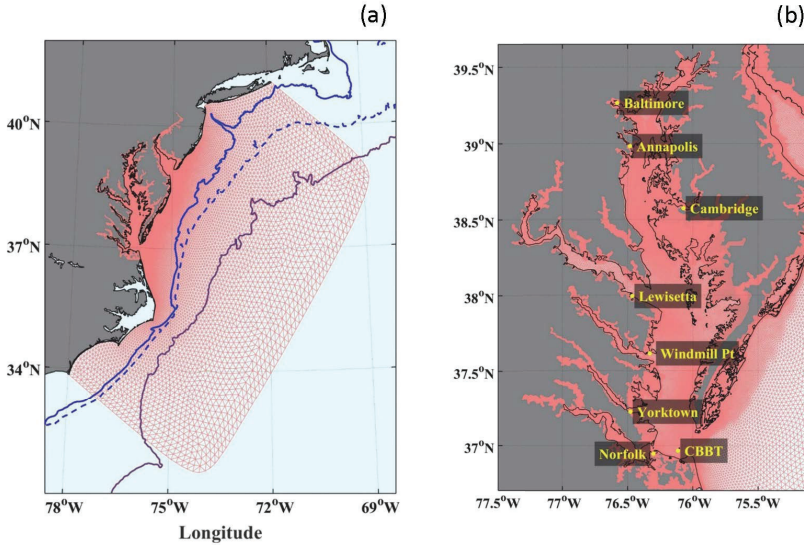[1] `https://imap.maryland.gov/Pages/lidar-dem-download-files.aspx`

FIGURE 4.2: (a) FVCOM model grids (red). (b) Zoomed-in view of FVCOM grids over Chesapeake Bay and the surrounding coastal plains.

2009). Raw elevation and bathymetry data referenced to different vertical datum are converted to the same vertical coordinate system (NAVD88) using the V-Datum program (Lee et al, 2017, Yang et al, 2008). Wetting and drying of grid cells is implemented to simulate overland inundation. FVCOM uses a point treatment technique in which numerical grids consist of wet and dry points with a boundary defined as an interface line between the water and land, respectively (Chen et al, 2011). A grid is treated as a wet point when the water depth exceeds the threshold h_c (set to be 5 cm in our model).

4.2.2   Design of numerical experiments

To project the impact of sea level rise on high tide flooding in 2050 and 2100, we make use of the IPCC AR5. The IPCC AR5 projections are based on a set of greenhouse gas concentration scenarios called Representative Concentration Pathways that reflect the updated greenhouse gas emission reduction possibilities and climate change stabilization goals (Moss et al, 2010, Van Vuuren et al, 2011). Under RCP 2.6 (Paris Agreement), emissions begin to decline now and become net zero later in the century, thus offering a reasonably good probability of keeping the increase in global mean temperature to less than 2 °C above pre-industrial levels in line with the Paris Climate Agreement. Under RCP 4.5 (Stabilized Emissions), emissions stabilize around their current levels slowly and then begin to decline after 2050. Under RCP 8.5 (Growing Emissions),

emissions continue to grow until the end of the century. We selected RCP 4.5 and 8.5, representative of medium (delayed action) and high (growing) emission scenarios, respectively.

At the offshore boundary, the FVCOM model was forced with the projected increase in the mean sea level superimposed onto the astronomical tides. This is a simplified representation of the sea level rise, which changes coastlines gradually, but previous studies by Bilskie et al (2016) and Ross et al (2017) suggested that forcing these sea level rise projections at the offshore boundary of a regional ocean model produces essentially the same results as more elaborate modeling approaches in which land subsidence and sea level rise are accounted for through bathymetry changes. The sea level projections used at the offshore boundary are based on the averages over the entire Chesapeake Bay, as regional differences in the future sea level rise projections are much smaller than the projected changes themselves (Kopp et al, 2014, Figures 4.1c and 4.1d). About 25% of the Chesapeake Bay shoreline is hardened, but these structures mostly use shoreline stabilization techniques such as riprap and bulkheading and do not provide much protection against flooding (Palinkas et al, 2018, Patrick et al, 2014). These small engineered structures are not resolved in the FVCOM model.

For each RCP scenario (RCP 4.5 or RCP 8.5) and for both 2050 and 2100, we considered the median (50%), the likely range (17%–83%) and very likely range (5%–95%) of the relative sea level rise projections (Kopp et al, 2014). A total of 20 numerical experiments were conducted.

4.2.3   Inundation impact analysis

Google Map and Google Earth are used to visualize inundations over the land areas surrounding Chesapeake Bay, including Annapolis, Baltimore, and Dorchester County in Maryland. Water level data from FVCOM were imported and overlaid on Google Map and Google Earth. Google Earth allows users to add and view 3D buildings, thus enabling 3D views of inundations over buildings and structures. Inundation depths are obtained by subtracting the LIDAR digital elevation data from the water level in each grid cell. The result is a wet/dry profile of inundation. To improve the accuracy of the profile, a layer representing buildings is used as a mask if one is available for the local jurisdiction. The resulting grid is then converted into vector polygons and stored in the geodatabase. The polygons in the geodatabase can be converted into KML files.

The inundation analysis focused on three local regions. Dorchester County was chosen as a representative rural site (Figure 4.3a). It is the largest county in Maryland and has a total area of 983 square miles (2550 km^2), including land areas of 1400 km^2 and water areas of 1140 km^2. According to the census in 2010, the county had a population of 32,618 and a population density of 55 people per square mile. There were 14,681 housing units at an average density of 26 per square mile, with the average home value of $188,000. The City of
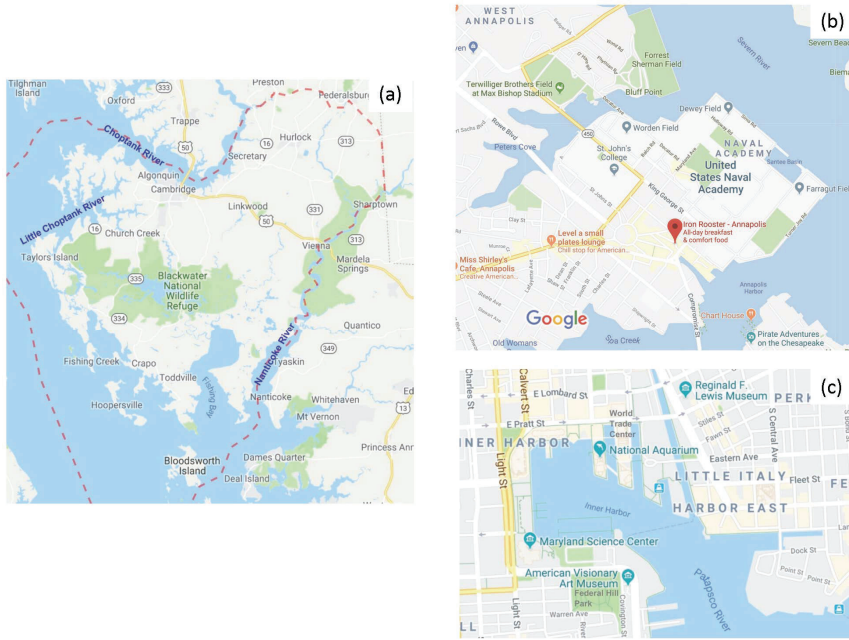
FIGURE 4.3: Maps of Dorchester County (a), downtown Annapolis (b), and Baltimore (c), Maryland.

Annapolis is the capital of the state of Maryland (Figure 4.3b). Its population was estimated to be 38,394 by the 2010 census. The population density was 5350 inhabitants per square mile. There were 17,850 housing units at an average density of 2485 per square mile. Annapolis is home to the US Naval Academy and many historical buildings such as the Maryland State House. The City of Baltimore was chosen as a representative urban site (Figure 4.3c). It is the largest city in Maryland, with a population of 2.81 million in the Baltimore metropolitan area. Baltimore is densely populated, with approximately 7671 people per square mile. Baltimore has about 50,800 firms where many of these firms and businesses are located on or near the waterfront. A majority of the properties in downtown Baltimore are commercial buildings.

4.3   Results

The probabilistic projections for high tidal flooding in 2050 and 2100 are presented for RCP 4.5 and 8.5. The Bay-wide response is presented first, followed by detailed analyses on Dorchester County, Annapolis, and Baltimore.

4.3.1 Bay-wide response

Figure 4.4 shows the projected inundated areas at high tide over the entire region of Chesapeake Bay in 2050. The Eastern Shore of Maryland and Virginia as well as the Atlantic coast of Delmarva Peninsula are the two regions most vulnerable to inundation. However, the extent of the flooding depends on the climate change scenario and projected relative sea level rise within each scenario. The median projection corresponds to the 50% probability that high tide will flood the areas (the middle column). The projected flooded areas for the 17% and 83% probability represent the likely range where the actual water boundary will lie between the contours of the two projections. The flooded areas for the 5% and 95% probability represent the very likely range for the high tide flooding. For example, land areas outside the flooded areas marked in the rightmost column will have less than a 5% chance of getting flooded in 2050. On the other hand, there is less than a 5% chance that the flooded areas will be smaller than those marked in the leftmost column in 2050. When the flooded areas are summed up over the entire Chesapeake Bay region, there is a 50% probability that the total inundated areas exceed 1285 km^2 under RCP 4.5 and 1303 km^2 under RCP 8.5 (Figures 4.6a and 4.6b). The difference between the two climate change scenarios is modest at the mid-21st century, as reflected in the small differences in the projected relative sea level rise between RCP 4.5 and 8.5 (Figures 4.1a and 4.1b). The likely range for the flooded areas, as defined by the 17% and 83% probability, lies between and 1,168/1,190 and 1,397/1,463 km^2 under RCP 4.5/8.5. The difference in the total inundated area between the upper and lower limit of the likely range is
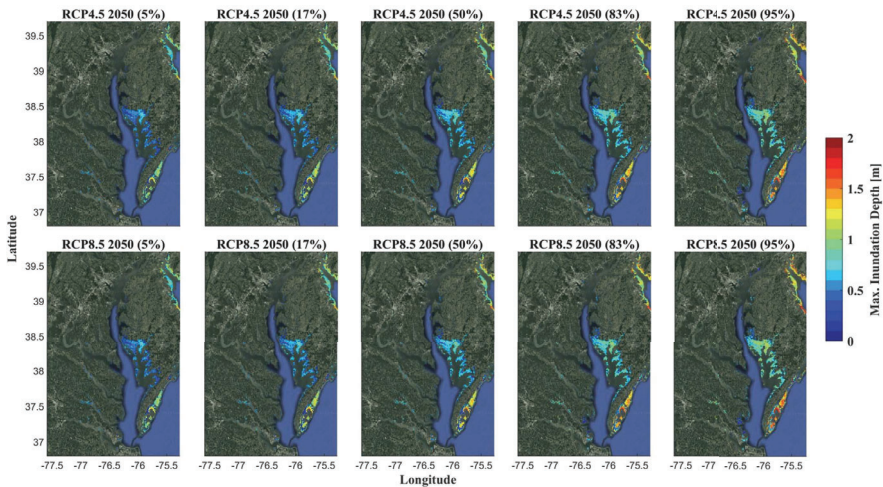

FIGURE 4.4: Probabilistic projections of inundated areas over Chesapeake Bay at 2050 under climate change scenarios RCP 4.5 and RCP 8.5.
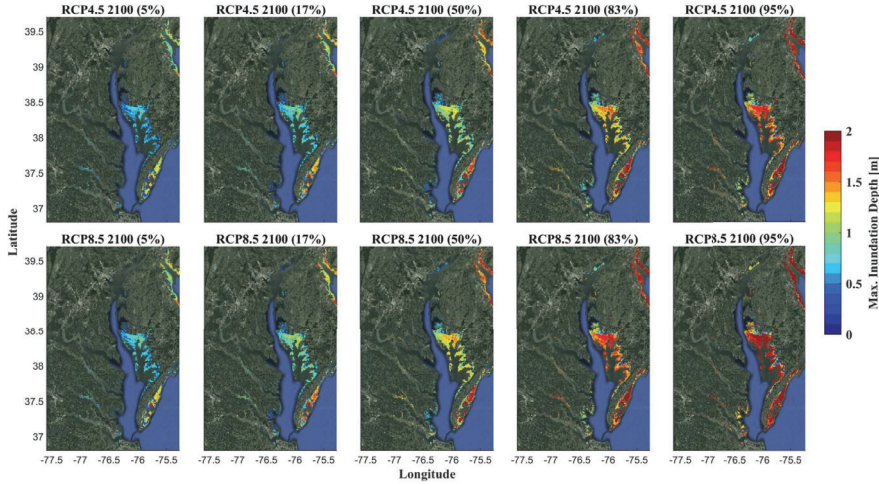
FIGURE 4.5: Probabilistic projections of inundated areas over Chesapeake Bay at 2100 under climate change scenarios RCP 4.5 and RCP 8.5.

about 20%, even though the difference in the relative sea level rise reaches 100% (0.32 m versus 0.68 m). The inundation depends not only on the sea level rise but also on how land topography varies in low-lying areas, such that 100% increase in the relative sea level rise only translates to a 20% increase in the inundated areas around the Chesapeake Bay. The very likely range for the flooded areas, as defined by the 5% and 95% probability, lies between and 1085/1099 and 1540/1594 km^2 under RCP 4.5/8.5. The total surface area of Chesapeake Bay is currently estimated to be 11,600 km^2. Therefore, the additional flooded areas in 2050 represent 9%–14% expansion in the surface water of the estuary, with the median projection at 11%.

   The inundated areas in 2100 show large spreads between the two climate change scenarios and among different probabilistic projections of the relative sea level rise, although the most vulnerable areas still lie on the Eastern Shore of Maryland and Virginia and the Atlantic Coast of Delmarva Peninsula (Figure 4.5). Under the median projection (50% probability) of RCP 4.5/8.5, a total of 1757/1912 km^2 are projected to be flooded by high tide in 2100 (Figures 4.6c and 4.6d). Compared with the median projections for 2050, this presents 37%/46% expansion of the inundated area around Chesapeake Bay under RCP 4.5/8.5. There is a much larger spread in the likely range: it lies between and 1489/1642 and 2012/2241 km^2 under RCP 4.5/8.5, amounting to 35%–36% difference in the total inundated area under each climate change scenario. Moreover, the total inundated area is 153–229 km^2 larger under RCP 8.5 than under RCP 4.5. The very likely range (5% to 95%) covers an
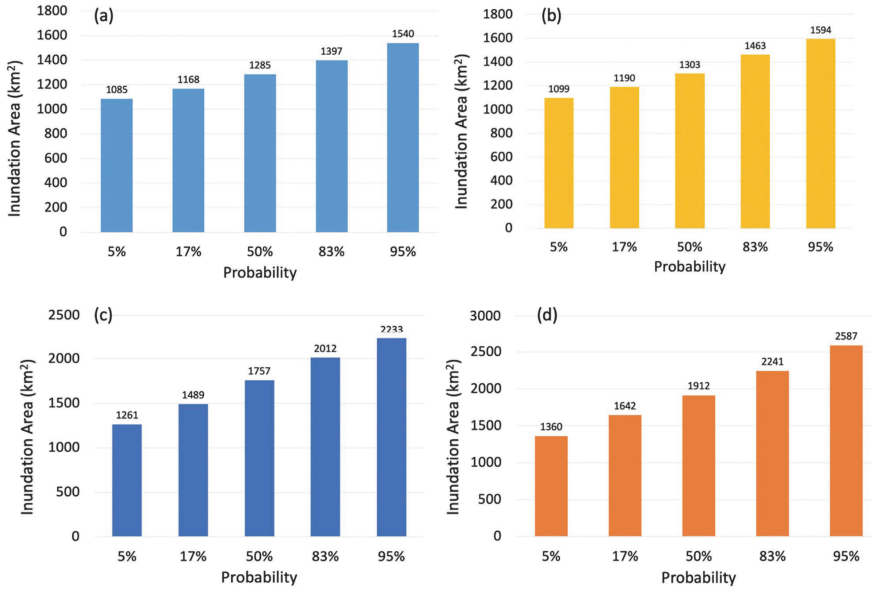
FIGURE 4.6: Total projected inundated areas over Chesapeake Bay at 2050 (a)/(b) and 2100 (c)/(d) under climate change scenarios RCP 4.5 and RCP 8.5.

even larger spread: ranging from 1261 to 2233 km^2 under RCP 4.5 and 1360 to 2587 km^2 under RCP 8.5.

4.3.2   Dorchester County

Figure 4.7 shows the inundated areas in Dorchester County at high tide in 2050. A large swath of land areas in southern Dorchester County will be flooded under most projections of the relative sea level rise. The inundated areas expand eastward and northward at higher water level projections. The median (50% probability) projection for the total inundated area in Dorchester County is nearly identical between RCP 4.5 and 8.5, at 581/589 km^2 (Figures 4.9a and 4.9b). This is equivalent to about 42% of the total land areas. In other words, over 40% of Dorchester County will be subjected to high tide flooding in 2050. The likely range of the flooded areas, as defined by the 17% and 83% probability, is between 540/547 and 619/632 km^2 under RCP 4.5/8.5. The very likely range of the flooded areas, as defined by the 5% and 95% probability, is between 508/513 to 654/671 km^2 under RCP 4.5/8.5. It is interesting to note the minor differences between RCP 4.5 and 8.5 and the narrow range of the projected areas as bracketed by different probabilistic
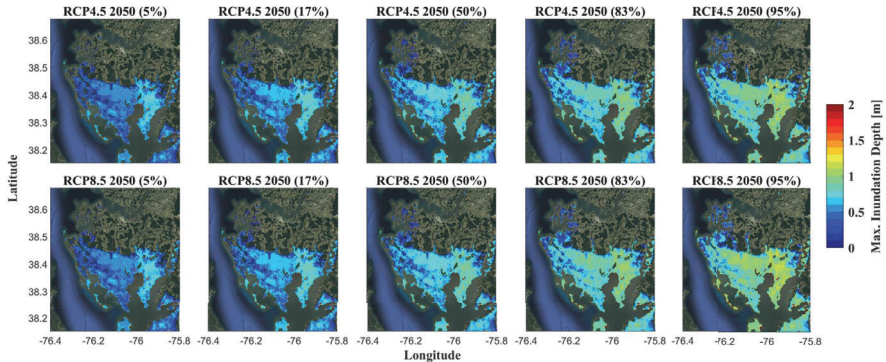
FIGURE 4.7: Probabilistic projections of inundated areas over Dorchester county at 2050 under climate change scenarios RCP 4.5 and RCP 8.5.

projections. This is a result of land topography over Dorchester County. The southern part of the county has low elevations but land elevation rises steeply further north and east. In contrast to the relative sensitivity of the inundated areas to climate change scenarios, the average inundation depth displays a wide range, reaching 0.45 m for the median projection and spanning 0.37 to 0.53 m for the likely range and 0.32 to 0.60 m for the very likely range (Figures 4.10a and 4.10b). Once again, the differences between RCP 4.5 and 8.5 are small at 2050.

By 2100, the flooded areas expand towards higher grounds in the northward direction (Figure 4.8). In particular, the northwest corner of Dorchester County, including the town of Cambridge, will be exposed to extensive tidal flooding. More flooding is projected under the higher end projections of the relative sea level rise, especially the 83% and 95% probabilistic projections. Moreover, there are significantly more flooded areas under RCP 8.5 than RCP 4.5. The median (50% probability) projection for the total inundated area in Dorchester County is 711/746 km^2 under RCP 4.5/8.5 (Figures 4.9c and 4.9d). This is 23%–27% larger than the corresponding projections in 2050. The likely range of the flooded areas is between 637/682 and 761/806 km^2 under RCP 4.5/8.5. The very likely range of the flooded areas is between 573/607 to 804/843 km^2 under RCP 4.5/8.5. Unlike 2050, there are significant differences in the total inundated areas between RCP 4.5 and 8.5. This reflects a wider range in the projected relative sea level rise rates in 2100 (Figures 4.1a and 4.1b), as well as the fact that higher water levels are now reaching new areas in the northwest corner of Dorchester County. There is 5% probability that over 60% of Dorchester County will be lost to tidal flooding and sea level rise in 2100 under the RCP 8.5 (business as usual) climate change scenario, with huge implications for the coastal communities.
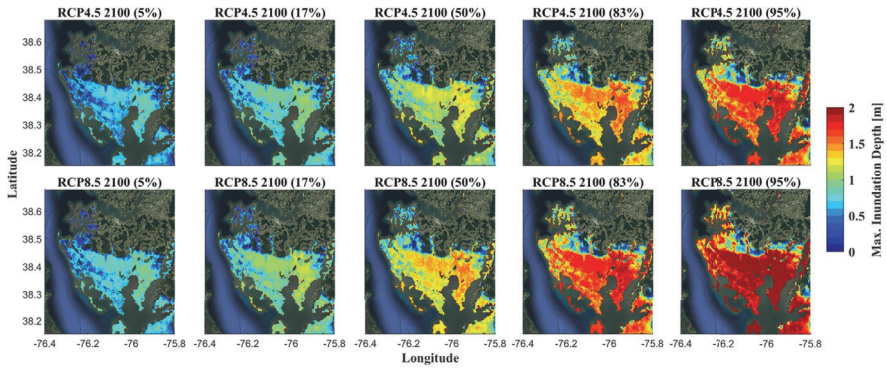
FIGURE 4.8: Probabilistic projections of inundated areas over Dorchester county at 2100 under climate change scenarios RCP 4.5 and RCP 8.5.
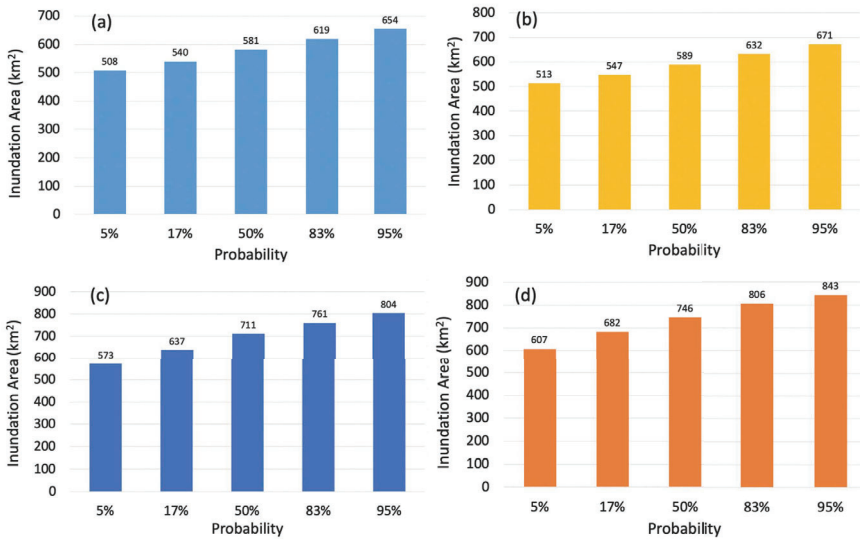

FIGURE 4.9: Total projected inundated areas over Dorchester County at 2050 (a)/(b) and 2100 (c)/(d) under climate change scenarios RCP 4.5 and RCP 8.5.
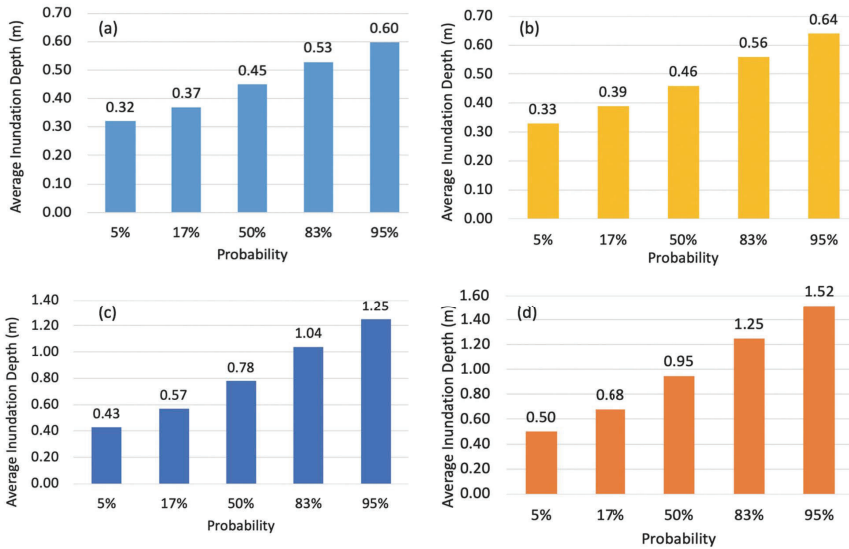
FIGURE 4.10: Probabilistic projections for average inundation depth over Dorchester County at 2050 (a)/(b) and 2100 (c)/(d) under climate change scenarios RCP 4.5 and RCP 8.5.

Such dire projections are compounded by the fact that the inundated areas will not simply be subject to minor nuisance flooding that is usually associated with tidal flooding, as shown in Figures 4.10c and 4.10d. The average inundation depth in Dorchester County is 0.78/0.95 m under the median projection of RCP 4.5/8.5. Unlike the total inundated areas which are relatively insensitive to different climate change scenarios and different probabilistic sea level rise projections, the average inundation depth spans a wide range. Its likely range spans 0.57–1.04 m and very likely range spans 0.43–1.25 m under RCP 4.5. Similarly, its likely ranges span 0.68–1.25 m and very likely range spans 0.50–1.52 m under RCP 8.5. At water depths 0.8–1.5 m, it would be impossible for residents to live in those areas. Even at the lower end projections, a water depth of 0.4–0.5 m would pose tremendous challenges for the livelihood of coastal communities.

4.3.3   Annapolis and Baltimore

Unlike the flat coastal plains on the eastern shore, the City of Annapolis has relatively steep topographic changes. Most of the tidal flooding areas are limited to the downtown waterfront areas and US Naval Academy (Figures 4.11 and 4.3b). At the upper end (83% and 95% probability) projections for 2100 under either RCP 4.5 or RCP 8.5, a large part of those areas
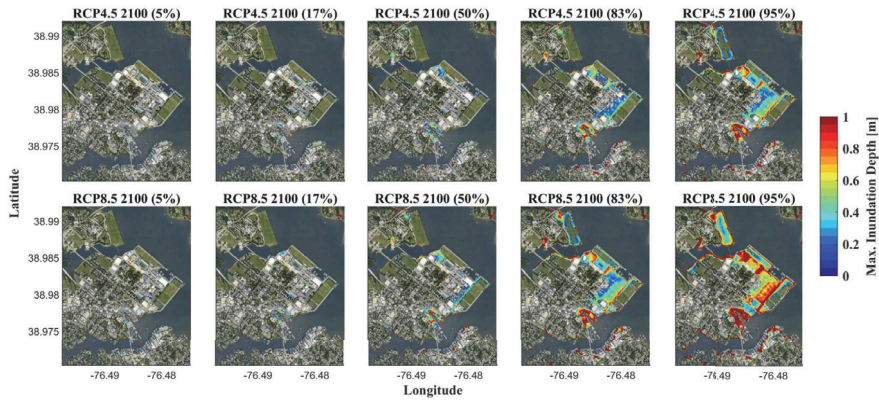
FIGURE 4.11: Probabilistic projections of inundated areas over City of Annapolis at 2100 under climate change scenarios RCP 4.5 and RCP 8.5.

will be under water. Many low-lying coastlines along the two creeks off the Sevens River will also subject to tidal flooding. In comparison, little areas will be flooded at high tide at the lower-end projections of the relative sea level rise. Only the downtown dock and a small part of the Naval Academy will be flooded in 2100 under the median projection of RCP 4.5 and 8.5. In terms of the total inundated areas for Annapolis, it only adds up to about 9000 m^2 in the median RCP 4.5 projection for 2050 and ranges from 5500 to 15,300 m^2 for the likely range (Figure 4.12a). The total flooded areas are only marginally higher under RCP 8.5 (Figure 4.12b). However, the average water depth in the flooded areas is about 0.45 m in all scenarios (Figures 4.13a and 4.13b), thus posing serious challenges for access and usage. Overall, these are relatively small flooding damages. In 2100, the total inundated area expands by 10–30 times (Figures 4.12c and 4.12d). The median projection reaches 90,000/16,500 m^2 under RCP4.5/8.5. There are wide spreads in the probabilistic projections for the inundated areas: the likely range spans from 19,600/42,500 to 256,000/506,500 m^2 under RCP 4.5/8.5. On the other hand, the average inundated depth for all scenarios falls into a narrow range of 0.44 to 0.51 m, with the exception of 0.70 m under the high-end projection (95%) of RCP 8.5 (Figures 4.13c and 4.13d). This offers an interesting contrast with the rural eastern shore where the inundated areas do not change much among the climate change scenarios, but the inundation depths are highly sensitive.

Tidal flooding in downtown Baltimore in 2100 is limited to the Inner Harbor, which is connected to Patapsco River, a tributary of Chesapeake Bay (Figure 4.3c). Hundreds of businesses are found in the downtown financial district, including skyscrapers like the Bank of America building and the Baltimore World Trade Center. Both Charles Street and Pratt Street are signifi-
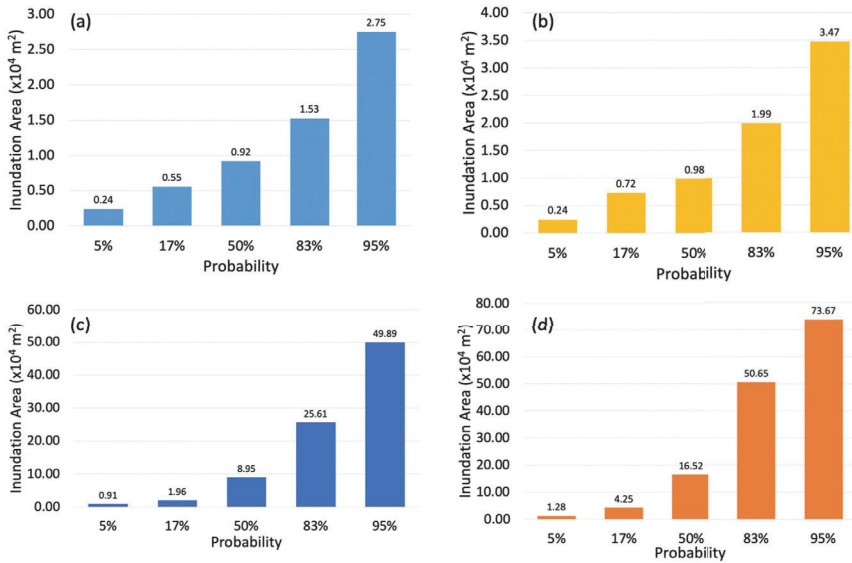
FIGURE 4.12: Total projected inundated areas over City of Annapolis at 2050 (a)/(b) and 2100 (c)/(d) under climate change scenarios RCP 4.5 and RCP 8.5.

cant avenues of commercial and cultural activity. To the northeast of the Inner Harbor lies in Fells Point and Little Italy featuring residential buildings and restaurants, with many low-lying areas. Figure 4.14 shows that a significant part of the downtown Inner Harbor and Little Italy districts will be flooded at high tide in 2100 under the higher end (the 83% and 95%) projections of RCP 4.5 and 8.5. No significant flooding is projected beyond the immediate boundary of the Inner Harbor under other scenarios.

4.4   Conclusions

Using the climate model projections to drive a regional ocean model, we have investigated how sea level rise affects high-tide flooding and coastal inundation in Chesapeake Bay. In 2050, there is a 50% probability that the total inundated areas will exceed $\sim$1300 km^2, equivalent to 11% of the current surface area of Chesapeake Bay. The likely range for the flooded areas, as defined by the 17% and 83% probability, lies between $\sim$1180 and 1420 km^2. In 2100, the projected inundated areas depend critically on the climate change scenario. Under the
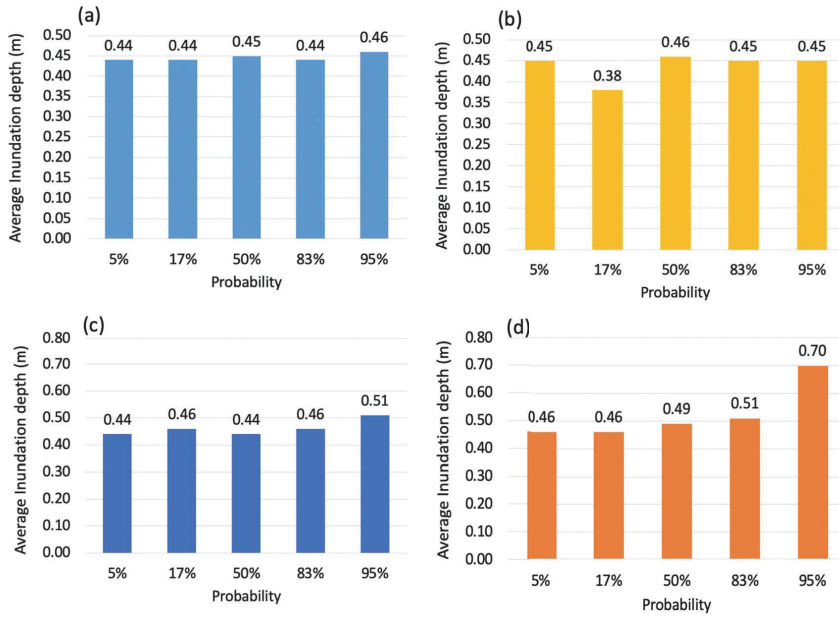
FIGURE 4.13: Probabilistic projections for average inundation depth over City of Annapolis at 2050 (a)/(b) and 2100 (c)/(d) under climate change scenarios RCP 4.5 and RCP 8.5.
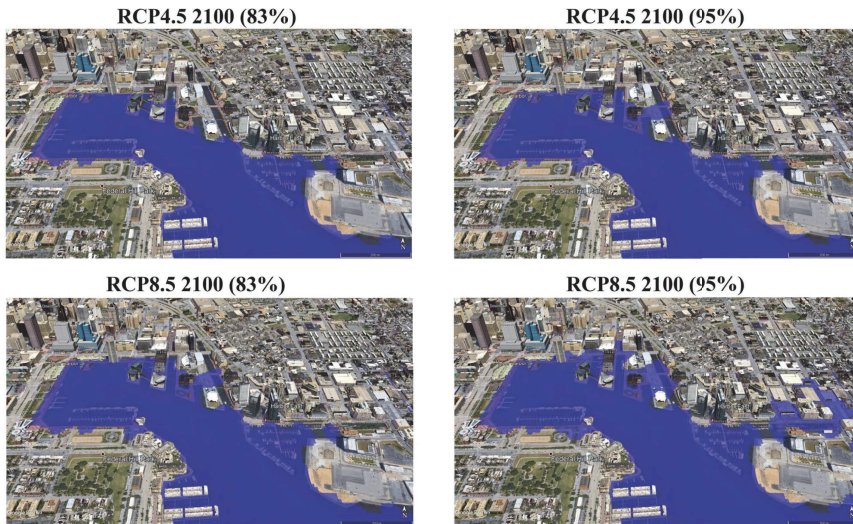

FIGURE 4.14: Projections of inundated areas over City of Baltimore at 2100 due to sea level rise under climate change scenarios RCP 4.5 and RCP 8.5.

median projection (50% probability) of RCP 4.5/8.5, a total of 1757/1912 km^2 are projected to be flooded. The likely range lies between and 1489/1642 and 2012/2241 km^2 under RCP 4.5/8.5, amounting to 35%–36% difference in the total inundated area under each climate change scenario. Moreover, the total inundated area is 153–229 km^2 larger under RCP 8.5 than under RCP 4.5.

The rural and urban areas show different responses to climate change, due to differences in land topography. Over the rural Dorchester County, the inundated areas show minor differences between different climate change scenarios and only moderate gains in 2100 than in 2050. However, the average inundation depth is ∼70%–100% higher in 2100 than in 2050. In comparison, the inundated areas in the City of Annapolis is projected to expand 10–30 times from 2050 to 2100: the median projection increases from 9800 m^2 in 2050 to 165,000 m^2 under RCP 8.5. On the other hand, the average inundated depth for all scenarios falls into a narrow range of 0.44 to 0.51 m, with the exception of 0.70 m under the high-end projection (95%) of RCP 8.5. In downtown Baltimore, no extensive tidal flooding is projected beyond the immediate neighborhood of the Inner Harbor except under the higher end projections of the relative sea level rise for 2100.

Although a number of inundation maps are available, none of them have adequately addressed the effects of climate change on coastal flooding. Projections of sea level rise onto low-lying land areas are mostly based on static images (e.g., bathtub approach) and do not consider dynamical processes of tides in rising seas. This study applies the latest research findings on sea level rise and develops dynamics-based inundation graphics that may better prepare coastal communities for the rising inundation risks in the 21st century. The State of Maryland has taken the threats of sea level rise seriously. In 2018, the Maryland General Assembly passed HB 1350/ SB 1006—Sea Level Rise Inundation and Coastal Flooding—Construction, Adaptation, and Mitigation, which was signed into law by the governor. Maryland expanded its "Coast Smart" siting and design criteria in order to better manage sea level rise and improve coastal adaptation efforts. The legislation also requires the state to establish a plan to adapt to saltwater intrusion, and to build criteria for hazard mitigation funding for sea level rise and coastal flooding. Coastal inundation projections described in this chapter may be useful to the state and local agencies tasked to execute the latest legislation on coastal flooding in Maryland.

Although this study focused on Chesapeake Bay and the State of Maryland, the same approach could be used to make probabilistic projections of overland inundation in other coastal regions. Kopp et al (2014) provided probabilistic sea level rise projections at locations around the world, and their projections could be used to drive models of other estuaries and coastal regions. Future model working could also consider a scenario of accelerating sea level rise in late 21st century that might be caused by rapid melt of the Antarctic ice (DeConto and Pollard, 2016, Kopp et al, 2017).

Future inundation studies will also need to consider the impact of climate change on storm surge flooding. Knutson et al (2013) conducted dynamic downscaling projections of the 21st-century Atlantic hurricane activity and found a significant increase in the frequency of intense storms. The combination of stronger storms and sea level rise will likely result in higher water levels and more extensive inundation in the future climate. Lin et al (2016) found that Hurricane-Sandy levels of flooding are becoming significantly more frequent in New York City compared to the scenario with sea level rise alone. Similarly, Zhang and Li (2019) found that a Category 2 storm like Hurricane Isabel (2013) will generate much higher sea levels in 2050 and 2100 due to the combined effect of sea level rise and warming ocean. To make a probabilistic prediction of storm-induced flooding, one would need to combine probabilistic sea level rise projections with model simulations of storms of different intensity, track, and size.

References

Amante C, Eakins BW (2009) ETOPO1 Global Relief Model converted to PanMap layer format. Boulder, CO

Bilskie MV, Hagen SC, Alizad K, Medeiros SC, Passeri DL, Needham HF, Cox A (2016) Dynamic simulation and numerical analysis of hurricane storm surge under sea level rise with geomorphologic changes along the northern Gulf of Mexico. Earth's Future 4(5):177–193

Boesch DF, Boicourt WC, Cullather RI, Ezer T, Galloway Jr GE, Johnson ZP, Kilbourne KH, Kirwan ML, Kopp RE, Land S, Li M, Nardin W, Sommerfield CK, Sweet WV (2018) Sea-level rise: projections for Maryland 2018. University of Maryland Center for Environmental Science, Cambridge, MD

Chen C, Liu H, Beardsley RC (2003) An unstructured grid, finite-volume, three-dimensional, primitive equations ocean model: application to coastal ocean and estuaries. Journal of Atmospheric and Oceanic Technology 20(1):159–186

Chen C, Beardsley RC, Cowles G (2006) An unstructured-grid, finite-volume coastal ocean model (FVCOM) system. Oceanography 19:78–89

Chen C, Beardsley RC, Cowles G, Qi J, Lai Z, Gao G, Stuebe D, Xu Q, Xue P, Ge J, Ji R, Hu S, Tian R, Huang H, Wu L, Lin H (2011) An unstructured-grid, finite-volume community ocean model FVCOM user manual, 3rd edn. SMAST/UMASSD, New Bedford, MA, USA

Church JA, Clark PU (2013) Climate change 2013: The physical science basis. In: Stocker TF, Qin D, Plattner GK, Tignor M, Allen SK, Boschung J, Nauels A, Xia Y, Bex V, Midgley PM (eds) Contribution of Working Group I to the Fifth Assessment Report of the Intergovernmental Panel on Climate Change, Cambridge University Press, Cambridge, UK, 1137–1216

Church JA, White NJ (2011) Sea-level rise from the late 19th to the early 21st century. Surveys in Geophysics 32(4–5):585–602

Dalton MM, Dello KD, Hawkins L, Mote PW, Rupp DE (2017) The third Oregon climate assessment report. Oregon Climate Change Research Institute, College of Earth, Ocean and Atmospheric Sciences, Oregon State University, Corvallis, OR

Dangendorf S, Marcos M, Wöppelmann G, Conrad CP, Frederikse T, Riva R (2017) Reassessment of 20th century global mean sea level rise. Proceedings of the National Academy of Sciences 114(23):5946–5951

DeConto RM, Pollard D (2016) Contribution of Antarctica to past and future sea-level rise. Nature 531(7596):591–597

Domingues R, Goni G, Baringer M, Volkov D (2018) What caused the accelerated sea level changes along the US East Coast during 2010–2015? Geophysical Research Letters 45(24):13–367

Egbert GD, Erofeeva SY (2002) Efficient inverse modeling of barotropic ocean tides. Journal of Atmospheric and Oceanic Technology 19(2):183–204

Ezer T, Atkinson LP, Corlett WB, Blanco JL (2013) Gulf Stream's induced sea level rise and variability along the US mid-Atlantic coast. Journal of Geophysical Research: Oceans 118(2):685–697

Flick RE, Murray JF, Ewing LC (2003) Trends in United States tidal datum statistics and tide range. Journal of Waterway, Port, Coastal, and Ocean Engineering 129(4):155–164

Garrett C (1972) Tidal resonance in the Bay of Fundy and Gulf of Maine. Nature 238(5365):441–443

Gesch DB (2009) Analysis of Lidar elevation data for improved identification and delineation of lands vulnerable to sea-level rise. Journal of Coastal Research 2009(10053):49–58

Ghanbari M, Arabi M, Obeysekera J, Sweet W (2019) A coherent statistical model for coastal flood frequency analysis under nonstationary sea level conditions. Earth's Future 7(2):162–177

Greenberg DA, Blanchard W, Smith B, Barrow E (2012) Climate change, mean sea level and high tides in the Bay of Fundy. Atmosphere–Ocean 50(3):261–276

Griggs G, Árvai J, Cayan D, DeConto R, Fox J, Fricker HA, Kopp RE, Tebaldi C, Whiteman EA (2017) Rising seas in California: an update on sea-level rise science. California Ocean Science Trust, Oakland, CA, USA

Hall GF, Hill DF, Horton BP, Engelhart SE, Peltier WR (2013) A high-resolution study of tides in the Delaware Bay: past conditions and future scenarios. Geophysical Research Letters 40(2):338–342

Hay CC, Morrow E, Kopp RE, Mitrovica JX (2015) Probabilistic reanalysis of twentieth-century sea-level rise. Nature 517(7535):481–484

Hinkel J, Lincke D, Vafeidis AT, Perrette M, Nicholls RJ, Tol RS, Marzeion B, Fettweis X, Ionescu C, Levermann A (2014) Coastal flood damage and adaptation costs under 21st century sea-level rise. Proceedings of the National Academy of Sciences 111(9):3292–3297

Holleman RC, Stacey MT (2014) Coupling of sea level rise, tidal amplification, and inundation. Journal of Physical Oceanography 44(5):1439–1455

Knutson TR, Sirutis JJ, Vecchi GA, Garner S, Zhao M, Kim HS, Bender M, Tuleya RE, Held IM, Villarini G (2013) Dynamical downscaling projections of twenty-first-century Atlantic hurricane activity: CMIP3 and CMIP5 model-based scenarios. Journal of Climate 26(17):6591–6617

Kopp RE (2013) Does the mid-Atlantic United States sea level acceleration hot spot reflect ocean dynamic variability? Geophysical Research Letters 40(15):3981–3985

Kopp RE, Horton RM, Little CM, Mitrovica JX, Oppenheimer M, Rasmussen D, Strauss BH, Tebaldi C (2014) Probabilistic 21st and 22nd century sea-level projections at a global network of tide-gauge sites. Earth's future 2(8):383–406

Kopp RE, DeConto RM, Bader DA, Horton RM, Hay CC, Kulp S, Oppenheimer M, Pllard D, Strauss BH (2017) Implications of Antarctic ice-cliff collapse and ice-shelf hydrofracturing mechanisms for sea-level projections. Earth's Future 5(12):1217–1233

Kulp S, Strauss BH (2017) Rapid escalation of coastal flood exposure in US municipalities from sea level rise. Climatic Change 142(3-4):477–489

Kulp SA, Strauss BH (2019) New elevation data triple estimates of global vulnerability to sea-level rise and coastal flooding. Nature Communications 10(1):1–12

Lee SB, Li M, Zhang F (2017) Impact of sea level rise on tidal range in Chesapeake and Delaware Bays. Journal of Geophysical Research: Oceans 122(5):3917–3938

Lin N, Kopp RE, Horton BP, Donnelly JP (2016) Hurricane Sandy's flood frequency increasing from year 1800 to 2100. Proceedings of the National Academy of Sciences 113(43):12071–12075

Miller KG, Kopp RE, Horton BP, Browning JV, Kemp AC (2013) A geological perspective on sea-level rise and its impacts along the US mid-Atlantic coast. Earth's Future 1(1):3–18

Mitchell M, Herschner CH, Herman JD, Schatt DE, Eggington E, Stiles S (2013) Recurrent flooding study for Tidewater Virginia. The Virginia Institute of Marine Science, Center for Coastal Resources Management, Old Dominion University, the Hampton Roads Planning District Commission, the City of Norfolk, the Accomack-Northampton Planning District Commission and Wetlands Watch, Richmond, VA

Moftakhari HR, AghaKouchak A, Sanders BF, Feldman DL, Sweet W, Matthew RA, Luke A (2015) Increased nuisance flooding along the coasts of the united states due to sea level rise: past and future. Geophysical Research Letters 42(22):9846–9852

Moss RH, Edmonds JA, Hibbard KA, Manning MR, Rose SK, Van Vuuren DP, Carter TR, Emori S, Kainuma M, Kram T, Meehl GA, Mitchell JFB, Nakicenovic N, Riahi K, Smith SJ, Stouffer RJ, Thomson AM, Weyant JP,

Wilbanks TJ (2010) The next generation of scenarios for climate change research and assessment. Nature 463(7282):747–756

Müller M, Arbic BK, Mitrovica JX (2011) Secular trends in ocean tides: observations and model results. Journal of Geophysical Research: Oceans 116:C05013

Palinkas CM, Sanford LP, Koch EW (2018) Influence of shoreline stabilization structures on the nearshore sedimentary environment in mesohaline Chesapeake Bay. Estuaries and Coasts 41(4):952–965

Patrick CJ, Weller DE, Li X, Ryder M (2014) Effects of shoreline alteration and other stressors on submerged aquatic vegetation in subestuaries of Chesapeake Bay and the mid-Atlantic coastal bays. Estuaries and Coasts 37(6):1516–1531

Ross AC, Najjar RG, Li M, Lee SB, Zhang F, Liu W (2017) Fingerprints of sea level rise on changing tides in the Chesapeake and Delaware Bays. Journal of Geophysical Research: Oceans 122(10):8102–8125

Sallenger AH, Doran KS, Howd PA (2012) Hotspot of accelerated sea-level rise on the Atlantic coast of North America. Nature Climate Change 2(12):884–888

Spanger-Siegfried E, Fitzpatrick M, Dahl K (2014) Encroaching tides: How sea level rise and tidal flooding threaten US East and Gulf Coast communities over the next 30 years. Union of Concerned Scientists, Cambridge, MA

Sweet WV, Park J (2014) From the extreme to the mean: Acceleration and tipping points of coastal inundation from sea level rise. Earth's Future 2(12):579–600

Van Vuuren DP, Edmonds J, Kainuma M, Riahi K, Thomson A, Hibbard K, Hurtt GC, Kram T, Krey V, Lamarque JF, Masui T, Meinshausen M, Nakicenovic N, Smith SJ, Rose SK (2011) The representative concentration pathways: an overview. Climatic Change 109(1–2):5

Yang Z, Myers EP, Wong AM, White SA (2008) VDatum for Chesapeake Bay, Delaware Bay, and adjacent coastal water areas tidal datums, and sea surface topography. Tech. Rep. NOS CS 15, NOAA, Silver Spring, MD

Zervas CE (2001) Sea level variations of the United States 1854–1999. Tech. Rep. NOS CO-OPS 36, NOAA, Silver Spring, MD, USA

Zervas CE (2009) Sea level variations of the United States, 1854-2006. Tech. Rep. NOS CO-OPS 53, NOAA, Silver Spring, MD, USA

Zhang F, Li M (2019) Impacts of ocean warming, sea level rise, and coastline management on storm surge in a semienclosed bay. Journal of Geophysical Research: Oceans 124(9):6498–6514

Zhong L, Li M, Foreman M (2008) Resonance and sea level variability in Chesapeake Bay. Continental Shelf Research 28(18):2565–2573